arXiv:1112.6350v1 [quant-ph] 29 Dec 2011

Double dark state cooling in a three level system

J. Cerrillo,[1, 2, *] A. Retzker,[2] and M. B. Plenio[2, 1]

[1] *QOLS, The Blackett Laboratory, Imperial College London, Prince Consort Rd., SW7 2BW, UK*
[2] *Institut für Theoretische Physik, Universität Ulm, D-89069 Ulm, Germany*

A detailed study of a robust and fast laser cooling scheme on a three level system is presented. A special laser configuration, applicable to trapped ions, atoms or cantilevers, designs a quantum interference that eliminates the blue sideband in addition to the carrier transition, thus excluding any heating process involving up to one-phonon processes. As a consequence cooling achieves vanishing phonon occupation up to first order in the Lamb-Dicke parameter expansion. Underlying this scheme is a combined action of two cooling schemes which makes the proposal very stable under fluctuations of the physical parameters such as laser intensity or detuning, making it a viable candidate for experimental implementation. Furthermore, it is considerably faster than existing ground state cooling schemes, overcoming one of the limitations of current quantum information processing implementations. Its suitability as a cooling scheme for several ions in a trap or for a cloud of atoms in a dipole trap is shown. This work extends the description of the "robust cooling scheme" introduced in [1].

I. INTRODUCTION

Processing quantum information commonly requires the initialization of a quantum register to a given pure state. In the case of trapped particles such as ions or atoms as well as for nanomechanical oscillators, this is usually achieved by means of ground state cooling. The success of quantum computational tasks, quantum information processing or quantum logic spectroscopy techniques are directly affected by the accuracy to which ground or initial states can be produced. Bose-Einstein condensation is reachable only after laser pre-cooling, and the very prolific field of quantum simulations relies on cooling schemes in many of its implementations.

The use of laser cooling schemes [2–4] has proven effective and useful in most of these fields, with the relevant exception of Bose-Einstein condensation, where many efforts have been directed towards the achievement of an all-optical means of obtaining quantum degeneracy [5]. Whether the particle is free or bound by an external potential dictates a fundamental distinction among different treatments. The idea underlying Doppler cooling [6] for free particles is related to sideband cooling [7, 8] for bound particles and similarly dark state cooling for free particles [9] has its counterpart for trapped ions [10].

At present sideband cooling is the method of choice for ground state cooling of trapped ions. The red sideband is preferentially addressed by detuning the laser light by the value of the trap frequency ν. This requires that the linewidth of the transition Γ allows for the necessary resolution. Hence this scheme only works in the so called strong confinement limit $\Gamma \ll \nu$. On instances where this limit is not satisfied, lower effective linewitdh might be engineered by means of laser couplings to other levels [11, 12]. Off-resonant heating processes (primarily carrier transition excitation, followed by blue sideband heating) limit its performance both in terms of cooling rate and final temperature. Its cooling rate is determined by the effective linewidth of the optical transition Γ_{eff} and the coupling strength of the laser light to the electronic levels, corresponding to the Rabi frequency Ω times the Lamb-Dicke parameter η. The minimum reachable phonon number is limited by $(\frac{\Gamma}{4\nu})^2$ in the case of very low driving.

The detrimental effect of the heating associated to the carrier transition can be overcome by means of dark state cooling schemes. Here, the destructive interference that generates Electromagnetically Induced Transparency (EIT) [13] cancels the resonant absorption. In a three level lambda system, the Raman coupling dresses the atomic states giving rise to one dark state and two excited states. By adjusting the detuning Δ and laser intensity Ω correctly, an effective coupling of the dark and the longest lived excited state can be achieved with a detuning equal to the trap frequency [14, 15]. The involvement of the dark state ensures the cancellation of the carrier transition, and the detuning adjustment enhances the red sideband transition with respect to blue sideband excitations. All in all, final ocupation numbers proportional to $\frac{\Gamma^2}{16|\Delta|^2}$ can be achieved, while the rate scales as $\eta^2\frac{\Omega^2}{\Gamma}$, thus beating sideband cooling for large detunings.

In the case of the Stark shift (SSh) cooling method [16], it is assumed that the Raman coupling present in the EIT scheme does not affect the mechanical degrees of freedom. Instead, this role is taken over by a direct and resonant coupling of the two lowest lying states. The dark and bright states with respect to the Raman coupling are precisely the dressed states of this new coupling, and its Stark shift can be adjusted through the coupling intensity [17]. If adjusted to the value of the trap frequency, a red sideband coupling is favored. This effectively transfers the mechanical energy to the bright state and then it is dissipated through its coupling to the excited state. Higher values of laser intensities can

---

* j.cerrillo@imperial.ac.uk

be applied with this proposal, allowing for an effectively faster operation of the scheme.

The limiting factor on both EIT and SSh coolings is the heating associated to the off-resonant blue sideband which, after the carrier transition, is the only heating process left up to first order phonon processes. For large Γ it is not possible to neglect the effect of the blue sideband, and cooling efficiency might be affected.

In [1] it has been shown that the blue sideband transition can be effectively canceled by the combination of both EIT and SSh cooling schemes. Both schemes are using the same dark state but different mechanisms, so that their combined effect on the same system is that of effectively canceling the blue sideband in addition to the carrier transition. Furthermore, the condition for cooling depends on the ratio of the Lamb-Dicke parameters of the couplings involved (rather than on the Rabi frequencies) thus making it a more experiment-friendly scheme.

In this paper we set out in detail the mechanism underlying the proposed scheme, with particular emphasis on possible systems for experimental implementation. The paper is organized as follows. In section II an explanation of the mechanism of the cooling scheme is presented, while the detailed explanation of the theoretical treatment is introduced in section III. An analysis of the properties of the scheme begins with section IV, where the robustness with respect to fluctuating experimental parameters is explained. The optimal cooling rate is found in section V. In section VI, two possible experimental implementations are set out, and the possibility of cooling the motion on more than one axis with the same scheme is presented in section VII. Section VIII deals with the effect that phase mismatch of the cooling fields would have on the efficiency of the scheme. The last two sections are devoted to the study of the applicability of this scheme to many body systems. On the one hand, in section IX the situation is considered where several ions sit on the same trap. On the other hand, in section X a cloud of dipole trapped atoms is assessed.

II. MECHANISM

Our proposal is designed for a 3-level lambda system of mass m which is trapped in a harmonic well of frequency ν. This can be an accurate model for an ion in an electromagnetic trap or an atom in a deep dipole trap. The three levels are coupled by means of an electric dipole interaction with running waves as shown in figure 1 and expressed in the following Hamiltonian:

$$\begin{aligned} H &= \nu b^\dagger b + \omega_e \left|e\right\rangle\left\langle e\right| + \omega_\uparrow \left|\uparrow\right\rangle\left\langle\uparrow\right| + \omega_\downarrow \left|\downarrow\right\rangle\left\langle\downarrow\right| \\ &+ \Omega_A \sigma_x^{(e,\uparrow)} \cos\left(\omega_A t + k_A x\right) \\ &+ \Omega_A \sigma_x^{(e,\downarrow)} \cos\left(\omega_A^* t - k_A x\right) \\ &+ \Omega_B \sigma_x^{(\uparrow,\downarrow)} \cos\left(\omega_B t + k_B x\right), \end{aligned} \tag{1}$$

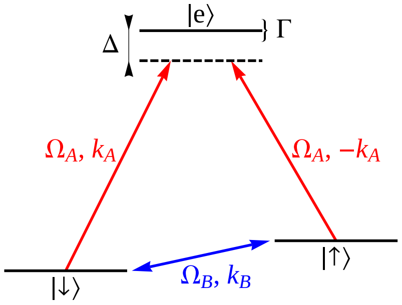

FIG. 1. A 3-level electronic system consisting of $\left|\uparrow\right\rangle$ and $\left|\downarrow\right\rangle$ and an excited state $\left|e\right\rangle$ which dissipates energy at rate Γ. The lower levels are coupled to $\left|e\right\rangle$ by a pair of Raman beams under a detuning Δ whose Rabi frequencies are Ω_A and wavevector projection on the cooling axis k_A of opposite sign (this may be achieved, e.g., by counterpropagating beams). $\left|\uparrow\right\rangle$ and $\left|\downarrow\right\rangle$ are directly coupled by a beam of Rabi frequency Ω_B and wavevector projection k_B.

where $\sigma_x^{(a,b)} = \left|a\right\rangle\left\langle b\right| + \left|b\right\rangle\left\langle a\right|$, $\Omega_{A,B}$ are the Rabi frequencies of the respective laser couplings, $\omega_{e,\uparrow,\downarrow}$ are the energy of the respective levels and $\omega_{A,B}^{(*)}$ are the frequencies of each laser. The metastable state $\left|\uparrow\right\rangle$ and the ground state $\left|\downarrow\right\rangle$ are considered to be infinitely lived, so the only dissipative state is $\left|e\right\rangle$.

This time dependent Hamiltonian can be simplified by moving to an interaction picture with respect to the appropriately detuned energy terms of the internal degrees of freedom. This requires the definition $\Delta = \omega_e - \omega_\uparrow - \omega_A = \omega_e - \omega_\downarrow - \omega_A^*$ and setting $\omega_\uparrow - \omega_\downarrow = \omega_B$. High frequency terms are dropped under a rotating wave approximation. It is useful to express each wavevector projection in terms of its corresponding Lamb-Dicke parameter following the definition $\eta = \frac{1}{\sqrt{2}} k x_0$, where $x_0 = \sqrt{\frac{\hbar}{m\nu}}$ is the zero point motion of the oscillator. Throughout the paper we consider the trapped system to be in the Lamb-Dicke regime, in which $\eta_A, \eta_B \ll 1$. In physical terms, this implies that the recoil energy gained in each photon emission is much smaller than the necessary energy to move one level in the trap, therefore processes involving phonon creation or annihilation are realized with small probability. An expansion of the Hamiltonian up to second order phonon processes is hence justified. Expressing the subspace spanning $\left\{\left|\uparrow\right\rangle, \left|\downarrow\right\rangle\right\}$ with the basis formed by $\left|+\right\rangle = \frac{1}{\sqrt{2}}\left(\left|\uparrow\right\rangle + \left|\downarrow\right\rangle\right)$ and $\left|-\right\rangle = \frac{1}{\sqrt{2}}\left(\left|\uparrow\right\rangle - \left|\downarrow\right\rangle\right)$ the Hamiltonian can be split into the following 4 terms:

$$H = H_{tr} + H_{int} + V_{EIT} + V_{SSh}, \tag{2}$$

with

$$\begin{aligned} H_{tr} &= \nu b^\dagger b, \\ H_{int} &= \Delta \left| e \right\rangle \left\langle e \right|, \\ V_{EIT} &= \Omega_A \left[\frac{\sigma_x^{(e,+)}}{\sqrt{2}} + \eta_A \sigma_y^{(e,-)} \hat{q} \right], \\ V_{SSh} &= \frac{\Omega_B}{\sqrt{2}} \left[\frac{\sigma_z^{(+,-)}}{\sqrt{2}} + \eta_B \sigma_y^{(+,-)} \hat{q} \right]; \end{aligned} \tag{3}$$

where $\sigma_z^{(a,b)} = \left| a \right\rangle \left\langle a \right| - \left| b \right\rangle \left\langle b \right|$, $\sigma_y^{(a,b)} = i \left| a \right\rangle \left\langle b \right| - i \left| b \right\rangle \left\langle a \right|$ and $\hat{q} = \frac{1}{\sqrt{2}}(b + b^\dagger)$. V_{EIT} and V_{SSh} are also refered to as the A and B couplings respectively. This Hamiltonian can be regarded as a combination of those describing the reversible dynamics of EIT and SSh coolings as expressed by

$$H_{EIT} = \nu b^\dagger b + \Delta \left| e \right\rangle \left\langle e \right| + \Omega_A \left[\frac{\sigma_x^{(e,+)}}{\sqrt{2}} + \eta_A \sigma_y^{(e,-)} \hat{q} \right] \tag{4}$$

and

$$\begin{aligned} H_{SSh} = \nu b^\dagger b + \Delta \left| e \right\rangle \left\langle e \right| + \frac{\Omega_A}{\sqrt{2}} \sigma_x^{(e,+)} \\ + \frac{\Omega_B}{\sqrt{2}} \left[\frac{\sigma_z^{(+,-)}}{\sqrt{2}} + \eta_B \sigma_y^{(+,-)} \hat{q} \right]. \end{aligned} \tag{5}$$

In the EIT case, the cooling transition is $\left| - \right\rangle \leftrightarrow \left| e \right\rangle$. There is no direct carrier transition driving it, only a combination of a blue and a red sideband expressed by the last term in (4). After diagonalization of the second and third terms, the values of Ω_A and Δ can be adjusted so that the detuning to one of the resulting dressed states matches the value of the trap frequency. In this way, the only process under resonance will be the red sideband to the resonant dressed state, and all other opto-mechanical processes will be off-resonant, including the two photon processes coupling $\left| \uparrow \right\rangle$ and $\left| \downarrow \right\rangle$. In the limit of large Δ, though, these two photon processes would gain in relevance.

The situation is similar in the SSh case. This time the cooling transition is $\left| - \right\rangle \leftrightarrow \left| + \right\rangle$. The carrier coupling between $\left| \uparrow \right\rangle$ and $\left| \downarrow \right\rangle$ transforms into a Stark shift in the $\left| + \right\rangle$ and $\left| - \right\rangle$ picture. This Stark shift can be adjusted to the value of the trap frequency so that again the red sideband is in resonance and the blue sideband is not.

This presents us with a Hamiltonian capable of performing two cooling schemes that apply to the same system and that operate by means of independent mechanisms. Both can be combined so that the only heating process remaining in both cooling transitions, namely the blue sideband, is canceled. In a master equation description spanning only up to one phonon processes, this amounts to only cooling processes being present; therefore the steady state of the system must be one with zero temperature, i. e. a pure state.

A. Derivation of the Steady State

It is possible to derive the form of the pure steady state of the system by analyzing the splitting of the Hamiltonian into EIT and SSh parts. What we want to find out is if there exists a steady state of the system that is pure and under which conditions this is so.

A steady state is such that the master equation vanishes. The coherent contribution of the Liouvillian vanishes for any eigenstate of the Hamiltonian, while the only atomic state involving incoherent dynamics is the excited state. This shows that a plausible instance of a pure steady state would be an eigenstate of the Hamiltonian with vanishing overlap with the excited state.

The only part of the Hamiltonian coupling the state $\left| e \right\rangle$ with the rest of the Hilbert space is the third term in eq. 3 (V_{EIT}) related to the EIT part of the cooling. Therefore, it is a condition that the eigenstate be dark to this term, i.e., $V_{EIT} \left| \Psi \right\rangle_{ss} = 0$. Since the system is within the Lamb-Dicke regime, perturbation theory is sufficient to solve it. Notationally, the Lamb-Dicke parameter order is indicated by a bracketed superscript. At leading order the equation becomes $\sigma_x^{(e,+)} \left| \Psi \right\rangle_{ss}^{(0)} = 0$, which implies $\left| \Psi \right\rangle_{ss}^{(0)} = \left| - \right\rangle \left| \phi \right\rangle_m$, with $\left| \phi \right\rangle_m$ an undetermined state for the mechanical degrees of freedom. For the first order, $\sigma_x^{(e,+)} \left| \Psi \right\rangle_{ss}^{(1)} + \sqrt{2}\eta_A \sigma_y^{(e,-)} \hat{q} \left| \Psi \right\rangle_{ss}^{(0)} = 0$. This determines that $\left| \Psi \right\rangle_{ss}^{(1)} = -i\sqrt{2}\eta_A \left| + \right\rangle \left| \phi' \right\rangle_m$ where $\left| \phi' \right\rangle_m = \hat{q} \left| \phi \right\rangle_m$.

The eigenvalue equation for the rest of the Hamiltonian can now be applied to fully determine the state. In the zeroth order, the only term involving the mechanical degrees of freedom is the frequency term $H_{tr} = \nu b^\dagger b$. As a consequence, the mechanical part of the zeroth order eigenvalue must be a Fock state, so $\left| \Psi \right\rangle_{ss}^{(0)} = \left| - \right\rangle \left| n \right\rangle$ and $\sqrt{2} \left| \phi' \right\rangle_m = \sqrt{n} \left| n-1 \right\rangle + \sqrt{n+1} \left| n+1 \right\rangle$. The next order equation determines the value of n. Since $V_{SSh}^{(1)} \left| \Psi \right\rangle_{ss}^{(0)}$ is proportional to $\left| \Psi \right\rangle_{ss}^{(1)}$, the eigenvalue equation requires that $(H_{tr} + V_{SSh}^{(0)}) \left| \Psi \right\rangle_{ss}^{(1)}$ also be proportional to $\left| \Psi \right\rangle_{ss}^{(1)}$. This will happen for $\left| \phi' \right\rangle_m$ a Fock state as well. The only value of n for which both $\left| n \right\rangle$ and $\hat{q} \left| n \right\rangle$ are Fock states is $n = 0$.

The state $\left| \Psi \right\rangle_{ss}$ has been fully determined as $\left| - \right\rangle \left| 0 \right\rangle - i\eta_A \left| + \right\rangle \left| 1 \right\rangle$. Whether this is indeed an eigenstate of the Hamiltonian can be guaranteed perturbatively, but the eigenvalues at each perturbative order have to be equivalent. Since the eigenvalue obtained at zeroth order is $-\frac{\Omega_B}{2}$ and the one at first order is $\nu + \frac{\Omega_B}{2}(1 - \frac{\eta_B}{\eta_A})$, the following condition arises:

$$\frac{\eta_B}{\eta_A} = \frac{2\nu}{\Omega_B} + 2. \tag{6}$$

This ensures that $\left| \Psi \right\rangle_{ss}$ is the unique eigenstate of the Hamiltonian that is a steady state of the master equation at the same time. This condition balances the values of the Lamb-Dicke parameters with respect to the value of the laser intensity and is shown below to be very robust to fluctuations.

B. Double Interference

This scheme couples the double transition $|-\rangle \leftrightarrow |e\rangle$ and $|-\rangle \leftrightarrow |+\rangle$ to the mechanics of the particle to generate cooling. It has been shown that the state $|-\rangle$ is decoupled from the rest of the Hilbert space at zeroth order in the Lamb-Dicke expansion. This constitutes the first interference of the system, canceling any carrier heating in the cooling transition and isolating $|-\rangle$ as the zeroth order electronic steady state. The electronic degrees of freedom unperturbed by the motion are described by the Hamiltonian

$$H_{el} = H_{int} + V_{EIT}^{(0)} + V_{SSh}^{(0)} = \sum_{i=e,+} \delta_i |i\rangle \langle i| + \frac{\Omega_A}{\sqrt{2}} \sigma_x^{(e,+)}, \tag{7}$$

where, taking the level $|-\rangle$ as the origin of energies, δ_e corresponds to $\Delta + \frac{\Omega_B}{2}$ and δ_+ is just Ω_B. The Ω_A coupling dresses the excited and bright states into $|D_1\rangle$ and $|D_2\rangle$ in the form

$$|+\rangle = \cos\theta |D_1\rangle + \sin\theta |D_2\rangle, \tag{8}$$

$$|e\rangle = \sin\theta |D_1\rangle - \cos\theta |D_2\rangle, \tag{9}$$

where

$$\tan\theta = -\frac{\delta_e - \delta_+}{\sqrt{2}\Omega_A} + \sqrt{\left(\frac{\delta_e - \delta_+}{\sqrt{2}\Omega_A}\right)^2 + 1}. \tag{10}$$

The eigenfrequencies of the states are $\delta_{D_{1,2}} = \left(\delta_e + \delta_+ \mp \sqrt{2\Omega_A^2 + (\delta_e - \delta_+)^2}\right)/2$. Both dressed states are dissipative due to their finite overlap with the excited state. Their energy uncertainty is Lorentzian-shaped but each has a different width proportional to the overlap to $|e\rangle$. In terms of the unperturbed states, though, the coupling to the continuum is the addition or subtraction of two Lorentzians. The case of the excited state is particularly interesting, since the change in sign makes it couple with positive amplitude for high energies and with a negative one for small ones. This together with the always positive coupling of the bright state can be combined to generate an energy-selective interference. An excitation from the dark to the excited state will interfere with that to the bright state for a particular value of energy. This value can be selected to be precisely that canceling the blue sideband by correctly adjusting the experimental parameters, as is derived below.

Because the excited state couples to a continuum of energies, a complete description should involve the modes of electromagnetic radiation to which it couples, so that a state of the system is described by the infinitely degenerate energy subspaces $\{|i,n\rangle\}$ with i any of the electronic levels and n the number of photons in any of the infinitely many modes of the environment, from where degeneracy arises. This notation is not to be confused with that of previous section, where the second digit corresponded to the phononic number. Assuming the radiation modes other than those of the lasers are empty, the Hamiltonian above would involve the states $|i,0\rangle$ (which are not degenerate and can therefore be redefined $|i\rangle$). An additional two couplings $|e\rangle \leftrightarrow |+,1\rangle$ and $|e\rangle \leftrightarrow |-,1\rangle$ complete the description of the system.

The manifold $\{|+\rangle, |e\rangle, \{|+,1\rangle\}, \{|-,1\rangle\}\}$ together with the corresponding couplings can be diagonalized, so that this would define a new continuum $|k\rangle$ with eigenvalue k. It is then possible to derive the relationship (see Appendix A)

$$\langle e|k\rangle = \frac{\sqrt{2}}{\Omega_A} (k - \Omega_B) \langle +|k\rangle \tag{11}$$

This introduces a change of sign of the overlap for energies below that of the state $|+,0\rangle$, and the crossing is known as a "Fano resonance". This change of sign is essential for the emergence of the interference in the blue sideband interaction.

Indeed, the blue and red sideband interactions can be expressed as

$$V_{int} = V_{EIT}^{(1)} + V_{SSh}^{(1)} = \left(\eta_A \Omega_A \sigma_y^{e,-} + \eta_B \frac{\Omega_B}{\sqrt{2}} \sigma_y^{e,-}\right) \hat{q}. \tag{12}$$

To zeroth order we assume the electronic state of the system to be located always in $|-\rangle$. The interaction can hence be simplified to

$$\left(\eta_A \Omega_A |e\rangle + \eta_B \frac{\Omega_B}{\sqrt{2}} |+\rangle\right) \langle -| \hat{q}. \tag{13}$$

Note that the notation including the photons has been dropped. The levels $|e\rangle$ and $|+\rangle$ have been shown to be a superposition of free energy states $|k\rangle$. Energy conservation will force the system to preferentially perform the transitions $|k=\nu\rangle \langle -| a$ (the red sideband) and $|-\nu\rangle \langle -| a^\dagger$ (the blue sideband), as are depicted in Fig.(2). The strength of these two transitions for the current interaction operator are

$$\begin{aligned} &\left(\eta_A \frac{\Omega_A}{\sqrt{2}} \langle \nu|e\rangle + \eta_B \frac{\Omega_B}{2} \langle \nu|+\rangle\right) |\nu\rangle \langle -| a = \\ &\left(\eta_A (\nu - \Omega_B) + \eta_B \frac{\Omega_B}{2}\right) \langle \nu|+\rangle |\nu\rangle \langle -| a, \end{aligned} \tag{14}$$

and, similarly, for the blue sideband,

$$\left[-\eta_A (\Omega_B + \nu) + \eta_B \frac{\Omega_B}{2}\right] \langle -\nu|+\rangle |-\nu\rangle \langle -| a. \tag{15}$$

The blue sideband can be made to vanish if the equation $\eta_A (\Omega_B + \nu) - \eta_B \frac{\Omega_B}{2} = 0$ is satisfied. This condition coincides with Eq.(6), which guarantees that the steady state is a pure state. This indicates the equivalence of both requirements.

C. Fano Resonance

From equation (11) it is clear that there exists an energy eigenstate from the continuum $|k\rangle$ that is orthogo-

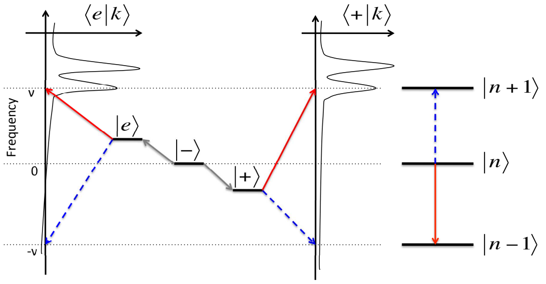

FIG. 2. Representation of the two first order processes in the system. In red (solid line) is the red sideband, which decreases the mechanical energy by one level while the internal degrees of freedom get excited to an energy of ν. The opposite process, in blue (dashed line), doesn't occur because the probability amplitude of the path through $|e\rangle$ and through $|e\rangle$ interfere with each other.

nal to $|e\rangle$. This is the phenomenon known as Fano resonance, and it offers an alternative way to implement a double interference in the system. For this, the coupling of the states $|\uparrow\rangle$ and $|\downarrow\rangle$ needs to be zero at first order in the Lamb Dicke expansion (i. e., $\eta_B = 0$) and the Rabi frequency needs to satisfy the resonance condition $\Omega_B = -\nu$. The nature of the interferences is therefore different as in the general case. For the Fano Resonance, the interference arises between the coupling of $|e\rangle$ and the continuum on the one hand and the coupling of $|+\rangle$ and $|e\rangle$ on the other hand. In the general case, the interference is between the laser couplings $|-\rangle \leftrightarrow |+\rangle$ and $|-\rangle \leftrightarrow |e\rangle$. Although the principle behind both alternatives is different, condition (6) contemplates both, since it gives the correct condition for Ω_B when $\eta_B = 0$.

The relevance of this alternative is paramount, since this might simplify considerably some experimental implementations. One of the challenges associated with the implementation of the scheme presented in this paper might be coupling $|\uparrow\rangle$ and $|\downarrow\rangle$ with a Lamb-Dicke parameter that is on the order of an optical one, since the energy difference between them is not of optical range. In section VI some options to generate optical Lamb-Dicke parameters are presented, involving two photon processes or magnetic gradients. The B coupling in the Fano resonance alternative doesn't need to involve the mechanical degrees of freedom, i.e., its Lamb-Dicke parameter can be negligible. Hence, non-optical means of coupling can be exploited, like microwave radiation or Zeeman effects. This makes the scheme more accessible where geometrical adjustments of the Lamb-Dicke parameters (described in section VI) are not possible. In addition, phase locking a microwave coupling to the laser coupling is experimentally accessible, making this option immune to the effects discussed in section VIII.

III. ANALYTICAL TREATMENT

Following the procedure in [18–20] the system under study is described using a master equation formalism, so that both the coherent dynamics and the dissipative nature of the excited level can be accounted for:

$$\frac{d\rho}{dt} = -i\,[H,\rho] + \mathcal{L}^d(\rho) = \mathcal{L}(\rho), \tag{16}$$

where ρ is the state of the system involving both the internal and the external degrees of freedom. The superoperator $\mathcal{L}^d$ is a Lindbladian for the two dissipative channels:

$$\mathcal{L}^d(\rho) = \sum_{i=\downarrow,\uparrow} \gamma_{e,i}(2\sigma_{i,e}\overline{\rho_{e,i}}\sigma_{e,i} - \rho\sigma_{e,e} - \sigma_{e,e}\rho), \tag{17}$$

where $\sigma_{j,k} = |j\rangle\langle k|$, the same rate $\gamma_{e,\downarrow} = \gamma_{e,\uparrow} = \Gamma$ is assumed for both channels and

$$\overline{\rho_{e,i}} = \frac{1}{2}\int_{-1}^{1} ds W(s) e^{ik_{e,i}xs}\rho e^{-ik_{e,i}xs} \tag{18}$$

accounts for the momentum transfer of $\hbar k_{e,i}$ in the event of a photon emission concomitant to the electronic decay from level $|e\rangle$ to level $|i\rangle$. $W(s) = \frac{3}{4}(1+s^2)$ is the angular distribution for a spontaneous emission of a dipole transition.

In the Lamb-Dicke approximation the Lindbladian can be expanded like the Hamiltonian, so that the first three terms of the whole Liouvillian $\mathcal{L}$ would appear

$$\begin{aligned}
\mathcal{L}_0(\rho) =& -i[\nu b^\dagger b, \rho] \\
& - i\left[\Delta\,|e\rangle\langle e| + \frac{\Omega_A}{\sqrt{2}}\sigma_x^{(e,+)} + \frac{\Omega_B}{2}\sigma_z^{(+,-)}, \rho\right] \\
& + \sum_{i=\downarrow,\uparrow}\gamma_{e,i}(2\sigma_{i,e}\rho\sigma_{e,i} - \rho\sigma_{e,e} - \sigma_{e,e}\rho) \\
=& \mathcal{L}_{0E}(\rho) + \mathcal{L}_{0I}(\rho), \\
\mathcal{L}_1(\rho) =& -i\left[\left(\frac{\Omega_A}{\sqrt{2}}\eta_A\sigma_y^{(e,-)} + \frac{\Omega_B}{2}\eta_B\sigma_y^{(+,-)}\right)\hat{q}, \rho\right], \\
\mathcal{L}_2(\rho) =& i\left[\left(\frac{\Omega_A}{\sqrt{2}}\eta_A^2\sigma_x^{(e,+)} + \frac{\Omega_B}{2}\eta_B^2\sigma_z^{(+,-)}\right)\hat{q}^2, \rho\right] \\
& + \alpha\sum_{i=\downarrow,\uparrow}\gamma_{e,i}\eta_i^2\sigma_{i,e}(2\hat{q}\rho\hat{q} + \hat{q}^2\rho + \rho\hat{q}^2)\sigma_{e,i},
\end{aligned} \tag{19}$$

where η_i is the Lamb-Dicke parameter corresponding to $k_{e,i}$. The zeroth order Liouvillian has been split in a part acting only on the external degrees of freedom $\mathcal{L}_{0E}$ and another one acting on the internal degrees of freedom $\mathcal{L}_{0I}$ to emphasize a lacking coupling among both at this order.

In the attempt to approximate a solution to the master equation, the theoretical approach in [11] is followed. Since the internal and external degrees of freedom are not coupled in the zeroth order Liouvillian, any steady state is separable, so that it can be expressed as a tensor product of electronic and mechanical states. Following the analytical procedures applied in the previous section, any zeroth order steady state is of the form $|-\rangle\,|n\rangle$ with $n = 0, 1, \ldots.$ The leading order Liouvillian has hence an infinitely degenerate subspace of steady states, i.e., of eigenvectors with an eigenvalue equal to zero. This eigenspace is connected by $\mathcal{L}_1$ and $\mathcal{L}_2$ to the rest of subspaces. To the extent that the cooling rate is slower than the dynamics of internal degrees of freedom and the trap frequency, it is possible to disregard the rest of the Hilbert space and focus on an effective master equation describing the dynamics of the phonon populations. This is achieved by projection of the global master Eq.16 to the null-eigenvalue subspace up to the second order.

$$\frac{d\mathcal{P}\rho}{dt} = [\mathcal{P}\mathcal{L}_2\mathcal{P} + \mathcal{P}\mathcal{L}_1(-\mathcal{L}_0^{-1})\mathcal{L}_1\mathcal{P}]\rho, \tag{20}$$

This can be used to derive a rate equation for the populations only:

$$\frac{d}{dt}\langle n\rangle = -(A_- - A_+)\langle n\rangle + A_+, \tag{21}$$

where A_+ and A_- are the heating and cooling rates respectively and they are a function of the system parameters with the condition $A_+(\nu) = A_-(-\nu)$. This offers an analytical prediction for the steady state mean occupation number $\langle n\rangle$ and for the rate of the cooling process W within the range of validity of the approximation:

$$\begin{aligned}\langle n\rangle &= \frac{A_+}{A_- - A_+};\\ W &= A_- - A_+.\end{aligned} \tag{22}$$

For the present scheme, the derivation of the rates gives the result

$$A_+ = [2\eta_A(\nu + \Omega_B) - \eta_B\Omega_B]^2/\mathcal{D}, \tag{23}$$

with $\Omega_A^2\Gamma\mathcal{D} = 4\Gamma^2(\nu+\delta_+)^2 + 4(\Omega_A^2/2-(\nu+\delta_+)(\nu+\delta_e))^2$. This rate will vanish exactly under the condition expressed in Eq.6, confirming the reasoning of Hamiltonian and coupling interference presented in section II. Vanishing heating rate indicates that the only remaining heating process in the system, namely the blue sideband, is being effectively canceled. This also implies that the cooling rate W is for that case equal to A_-.

IV. ROBUSTNESS

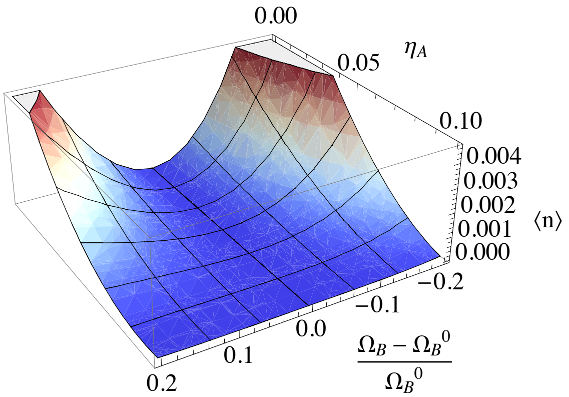

FIG. 3. Expected value of occupation $\langle n\rangle$ as a function of the Lamb-Dicke parameter η_A and of variations around the optimal Rabi frequency Ω_B^0, where it is shown how fluctuations have a worse effect as η_A vanishes, that is, as the Stark-shift cooling regime is approached ($\eta_B = 0.4$, $\Omega_A = 0.1\nu$).

The destructive interference between EIT and Stark-shift contribution is crucial for understanding the robustness of the scheme under fluctuating parameters. If the Rabi-frequencies deviate from Eq.6 by $\Delta\Omega_{A/B}$, the final population is affected by

$$\langle n\rangle \propto (\Delta\Omega_A)^4(\Delta\Omega_B)^2, \tag{24}$$

in contrast to the second order dependence as is usually the case. In other techniques such as SSh or EIT the resonance conditions do not necessarily match a population minimum and fluctuations can be very significant. As is exemplified in Fig.3, operation of Stark-shift only or EIT only cooling schemes suffer more from Rabi frequency fluctuations than the combination of both in the “robust cooling scheme”. This can act as an experimental protection to the performance of the cooling scheme, providing more certainty to the theoretical predictions also in a more realistic frame of fluctuating laser intensities.

Indeed, actual experimental application of EIT cooling yielded final population values of order 10^{-1}. The theoretically predicted value is lower of about an order of magnitude, indicating that a realistic prediction of the final result should take into account the uncertainty in the experimental parameters. Our analytical model predicts final populations of the order of 10^{-8} even for Rabi frequency fluctuations of about 2%, leaving thus ample room for experimental improvement.

The robustness of the system can be improved significantly if the Rabi frequency of the B coupling is set as close as possible to the value of the trapping frequency and Eq.6 is accordingly met. In this circumstance the contribution to fluctuations from the term $(\Delta\Omega_A)^4(\Delta\Omega_B)^2$ almost vanishes and the next term in the Taylor expansion takes over, thus yielding

$$\langle n\rangle \propto (\Delta\Omega_A)^4(\Delta\Omega_B)^4, \tag{25}$$

which ensures excellent stability and hence makes it arguably advisable, although not mandatory, to set the scheme to meet $\Omega_B = \nu$. As is shown below, this value is not optimal for cooling rate considerations, so a compromise between both is necessary.

V. COOLING RATE

The analytical prediction for the cooling rate derived above reads

$$W = \frac{4\eta_A^2\nu^2\Omega_A^2\Gamma}{\Gamma^2(\nu-\delta_+)^2+\left[\Omega_A^2/2-(\nu-\delta_+)\,(\nu-\delta_e)\right]^2}. \qquad (26)$$

This rate corresponds to the absorption probability at the trap frequency (A_-) since, under condition (6), the emission at that frequency (A_+) vanishes. The absorption spectrum has a peak for each of the dressed states $|D_1\rangle$ and $|D_2\rangle$, so the rate will be highest when the broader of the two resonances matches the trap frequency. The conditions $\delta_{D_2} = \nu$ corresponds to

$$\Omega_A^2 = 2(\nu-\delta_+)\,(\nu-\delta_e)\,, \qquad (27)$$

and the inequality $\delta_+ \geq \delta_e > \nu$ so that the resulting rate expression is

$$W = \frac{4\eta_A^2\nu^2\Omega_A^2}{\Gamma\,(\nu-\delta_+)^2}. \qquad (28)$$

The validity of this expression is constrained to the perturbative treatment applied here. The internal dynamics governed by $\Omega_i\eta_i$ must always be slower than the internal dynamics. Hence, it breaks down for cases where $\Omega_A \gg \delta_e, \delta_+$, since then it is $|D_1\rangle$ the broader dressed state. The singularity $\delta_+ = \nu$ is resolved as $\frac{8\eta_A^2\nu^2}{\Gamma}$, although it corresponds to vanishing Ω_A and is then of no interest. The validity of the expression is explored in Fig.(4) for a particular set of parameters, where it is shown how the analytical calculation matches the numerical simulation only for small values of Ω_A.

Placing the resonance at the value of the trap frequency imposes one condition on the parameters, but there are still enough degrees of freedom to lock the position of the second peak. The first order laser-motion interaction Eq.(12) generates two phonon processes when second order perturbation theory is invoked. In order to enhance this effect, one can place the peak at two times the trap frequency. The conditions $\delta_{D_2} = \nu$ and $\delta_{D_1} = 2\nu$ can then be simplified to

$$\delta_e + \delta_+ = 3\nu, \qquad (29)$$

$$(\delta_e - \delta_+)^2 + 2\Omega_A^2 = \nu^2. \qquad (30)$$

This and the fact that A_+ vanishes in this scheme allows for faster cooling rates as compared to schemes where this is not the case. As an example, the plot in Fig.(5) compares the cooling rate as a function of Ω_A for our scheme and EIT cooling. Because SSh is only slightly slower than our scheme makes its curve overlap and it can't be shown in the plot. Optimization of the values of both Rabi frequencies for $\Gamma = 15\nu$ and $\eta_B = 0.1$ can provide cooling rates of up to 0.06ν, whereas higher values for the Lamb-Dicke parameter makes it possible to accelerate the scheme to just one order of magnitude below the trap frequency.

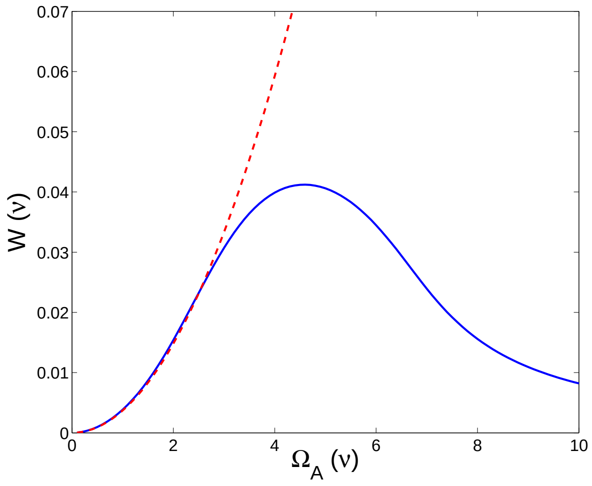

FIG. 4. Comparison of the cooling rate W obtained by means of numerical (solid blue line) or analytical (dashed red line) calculations as a function of the rabi frequency Ω_A ($\Gamma = 15\nu$, $\Omega_B = 1.3\nu$, $\eta_B = 0.1$). For large values of Ω_A the analytical result fails to predict the numerical values.

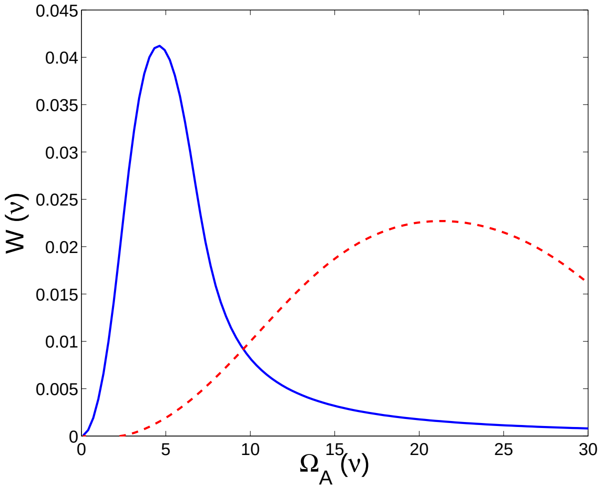

FIG. 5. Comparison of the numerical cooling rate W for our scheme (solid blue line) and EIT cooling (dashed red line) as a function of the rabi frequency Ω_A ($\Gamma = 15\nu$, $\Omega_B = 1.3\nu$, $\eta_B = 0.1$). The current scheme has in general a better performance already for smaller Rabi frequency values.

VI. EXPERIMENTAL IMPLEMENTATION

This proposal can be experimentally implemented in a number of different ways. Although the scheme applies to very general three level systems, we assume the ground level transition to be of microwave or rf order and the excited state to be at an optical distance above the ground level. The A coupling can hence be performed with two optical Raman laser beams, and the question remains then of how to perform the microwave coupling B. The scheme condition Eq.6 lays a constrain for the Lamb-Dicke parameter of coupling B, which has to be at least double that of coupling A. Another option is avoiding mechanical coupling of the ground state interaction ($\eta_B = 0$), following the "Fano resonance" alternative of the scheme. This simplifies the scheme in that a microwave coupling would be enough and locking it to the laser is experimentally accessible, making it resistant to phase effects discussed in section VIII. Two viable implementations are taken under consideration below, although they don't exhaust the range of possibilities.

A. Magnetic gradients

The direct driving of a microwave transition has an associated Lamb-Dicke parameters which is orders of magnitude smaller than that of an optical frequency. In order to increase its value, a magnetic gradient can be applied, as is set out in [21, 22]. In this system the magnetic gradients create a coupling of the following type:

$$\lambda\sigma_z(b + b^\dagger), \tag{31}$$

where λ is proportional to the gradient of the magnetic field and the two level system is driven using a microwave of the form $\Omega_d\sigma_x \cos\omega_d t$, where Ω_d corresponds to the Rabi frequency and ω_d to the angular frequency of the driving wave. After a Schrieffer-Wolff transformation the resulting Hamiltonian is exactly as in Eq.3 when the Rabi frequency is replaced by Ω_d and the Lamb-Dicke parameter is replaced by $\frac{\lambda}{\nu}$. The range of practically achievable values is comparable to that of optical transitions [21].

This scheme can be especially useful to cool nano scale resonators, by using the setup described in [23]. In this setup an NV center is coupled to a diamond cantilever, the coupling is performed by magnetic gradients resulting in the same Hamiltonian as described above. In cantilevers the speed of cooling is very important due to the finite Q value, which is a central factor limiting the attainable final temperatures at present. The high cooling rate achieved by the described scheme will result in lower final temperatures bringing us closer to the goal of reaching the quantum regime in cantilever systems.

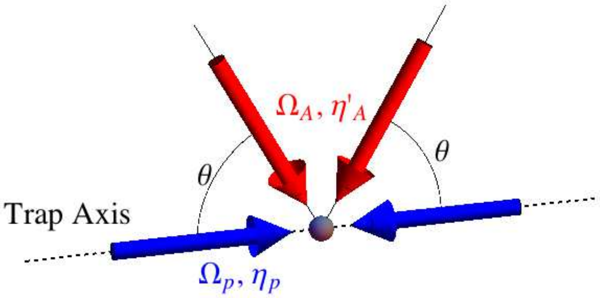

FIG. 6. Physical realization of Ω_A and Ω_B couplings, for cooling in the trap axis, as two Raman pair of beams characterized by their respective Rabi frequency Ω_A and Ω_p and their Lamb-Dicke parameters η'_A and η_p.

B. Highly detuned Raman beams

Alternatively, the ground states can be coupled by optical means, thus directly ensuring a Lamb-Dicke parameter of similar order as for coupling A. In order to do so, Raman beams with large single-photon detuning Δ' are envisaged to couple levels $|\uparrow\rangle$ and $|\downarrow\rangle$. As is shown in Fig.6 they have independent Rabi frequency Ω_p and Lamb-Dicke parameter η_p. The large detuning effectively decouples it from the excited state, unlike coupling A. Hence, adiabatic elimination of the upper level is possible and it yields the relationships between our effective parameters Ω_B and η_B and the physical values Ω_p and η_p. Its derivation is presented in appendix B, and it is found that $\Omega_B = \Omega_p/\Delta'$ and $\eta_B = 2\eta_p$ for sufficiently large detunings ($\Delta' \ll \nu$) and in the Lamb-Dicke regime. Meanwhile, the beams for the A couplings are tilted an angle θ with respect to the trap/cooling axis, so that $\eta_A = \eta'_A \cos\theta$. This provides us with an additional geometrical degree of freedom to adjust the ratio η_B to η_A.

Even though the detunings of each of the couplings are different, the fact that we are dealing with optical frequencies justifies $\eta'_A \simeq \eta_p$, and under this assumption $\frac{\eta_B}{\eta_A} = \frac{2}{\cos\theta}$. By relating this to the resonance Rabi frequency, $\cos\theta = \frac{\Omega_B}{\nu+\Omega_B}$, it is shown that the available angle range $\theta = [0, \frac{\pi}{2}]$ will span all possible values of Ω_B. If we choose the optimal point for the fluctuations about the value $\Omega_B = \nu$, the condition becomes $\eta_B/\eta_A = 4$, which corresponds to a layout where $\theta = 60^o$. A compromise with the cooling rate has to be reached, though, so that the optimal angle will be close but not exactly 60^o.

It may happen that the trap has very limited optical access so that θ is constrained to other non-optimal values. There is a way around this on the grounds that Δ' still constitutes a useful degree of freedom. Since it has no upper constrain, the B coupling can be performed with frequency doubled beams so that $\eta_p \simeq 2\eta_A$ and the optimal constrain is achieved already at $\theta = 0$.

Additionally, in cases where neither the geometrical configuration nor the detuning can be optimized, the aforementioned robustness of the scheme ensures excellent performance. Whether the cooling rate or the final temperature need to be improved, appropriate set of parameters can be found by numerical means. Usual experimental layouts of ion traps use vacuum chambers with windows at 22.5^o and/or 45^o from the trap axis, which generally allow for an angle range of about $\pm 10^o$. Assuming Δ' can't take values on the optical range, and taking 45^o as an operating value, the Lamb-Dicke parameter quotient becomes $\eta_B/\eta_A = 2\sqrt{2}$. Eq.6 can still be observed by adjusting Ω_B, and $\Omega_A = 0.6\nu$ and $\Delta \simeq 0$ optimizes the cooling rate for this condition. This final result can be improved depending on the particular values of the transition linewidth Γ. On the contrary, if the cooling rate is to be enhanced, Eq.6 will not be satisfied. In particular, for $\Omega_A \simeq 0.4\nu$, $\Omega_B \simeq 0.45\nu$ with 5% fluctuation and $\Delta \simeq -2\nu$ the population can still be as low as 10^{-3} while having a cooling rate faster than that of EIT cooling. Taking into account the fact that angles up to 55^o are accessible the cooling rate can still be improved by up to two orders of magnitude.

Actually, the implementation picture of a double pair of Raman beams makes both couplings totally interchangeable, allowing for further physical intuition. While a configuration of the two A beams perpendicular to the trap axis represents the Stark-shift cooling (disregarding Eq.6 and tuning $\Omega_B = \nu$), a value of $\theta = 0$ and the corresponding Rabi frequencies tuning is equivalent to EIT cooling. Any intermediate configuration realises an instance of Robust cooling. This picture is also very intuitive to understand how flexible the cooling scheme is regarding the cooling of the radial modes, since the addition of only two more laser beams in a suitable inclination with respect to the trap axis can cool down all three dimensions in the same Robust regime.

VII. MULTIAXIAL COOLING

So far one-dimensional cooling has been discussed. Nevertheless, the flexibility of the implementation of fig. (6) facilitates addressing more than one direction in the trap, so that multiaxial cooling can be achieved without adding any other beams to the scheme. In particular, two independent azimuthal angles constitute the necessary degrees of freedom to adapt the cooling for two perpendicular directions. The question remains whether the third direction will as well verify condition (6) and to which extent. This is in general not going to be the case, but even in this situation detuning degrees of freedom can be used to implement Raman sideband cooling to that axis.

In the case where traps have very limited access it is always possible to find an axis where cooling takes place. When two independent dimensions share the same trapping frequency it is always possible to find an axis for which the cooling condition is fulfilled. This is usually the case for the both radial modes in an ion trap. As long as the projection on the radial plane of couplings A and B corresponds to two pairs of counterpropagating beams θ-rotated from each other, it is possible to define an axis where the projection of the couplings fulfills the cooling condition. This axis can analytically be characterized by the definition of a new polar angle θ' as shown in Fig.7.

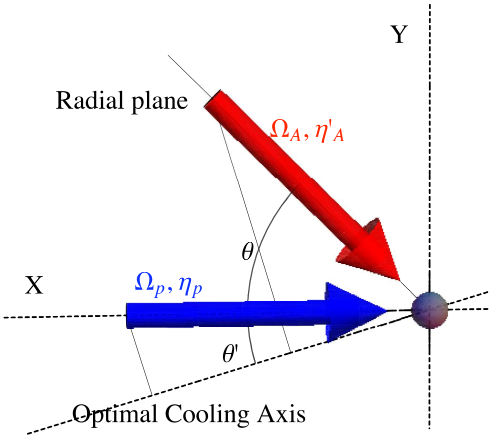

FIG. 7. Geometrical definition of angle θ' and representation of the projection of the two Lamb-Dicke parameters to the optimal cooling axis when $\eta'_A \simeq \eta_p$.

The ratio of Lamb-Dicke parameters A and B on any axis θ' of the plane is

$$\frac{\eta_B}{\eta_A} = \frac{2\cos\theta'}{\cos(\theta + \theta')} \tag{32}$$

The newly defined axis will fulfill the optimal cooling condition (6) for the angle

$$\theta' = \arctan\left(\frac{(\Omega_B + \nu)\cos\theta - \Omega_B}{(\Omega_B + \nu)\sin\theta}\right). \tag{33}$$

For any angle θ in the range $(0, \frac{\pi}{2})$ there always exists a solution in the range $(0, \frac{\pi}{2})$. Furthermore, it can be shown that the sum of both θ' and θ is never larger than $\pi/2$, so that geometrical considerations can be restricted to one quadrant.

Only geometrical degrees of freedom have been exhausted in this description. For traps with limited access also detuning degrees of freedom can be exploited in order to guarantee cooling in all three spatial directions.

VIII. PHASE EFFECTS

In view of an experimental implementation it is important to determine whether beam phase mismatches can be relevant to the performance of the scheme. Surprisingly enough, out of 4 beams used in the implementation

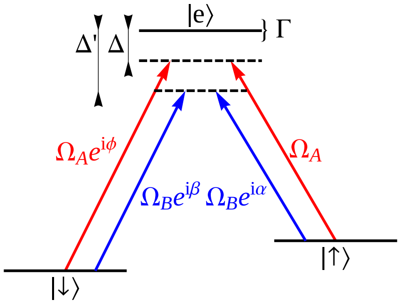

FIG. 8. All possible phase mismatches expressed with respect to the A coupling (red) between $|\uparrow\rangle$ and $|e\rangle$.

proposal a single phase mismatch can account for all the effects on the performance. To show this, it is helpful to define all possible phases, as in fig.8, with respect to the beam of coupling A between $|\uparrow\rangle$ and $|e\rangle$. The system would be oblivious to phase mismatch in the case where $\beta = 0$ and $\alpha = \phi$, i.e., to a global phase difference between beams coupling different ground states. This is so because one can always redefine the corresponding ground state so that it absorbs the same amount of phase in both beams.

Out of the pair of Raman beams performing the B coupling, only the difference of its phases survives in the effective microwave coupling between ground states. This effect leaves room for a redefinition of their phases so that $\alpha \to (\alpha - \beta)$ and $\beta \to 0$ is rather chosen. After the redefinition, the phase difference between both legs remains the same, i.e., the effective Hamiltonian is unchanged while the initial picture is simplified to a 2 phase system.

Now only the two beams coupling $|\downarrow\rangle$ to $|e\rangle$ have a non-zero phase. The redefinition $|\downarrow\rangle \to e^{-i(\alpha-\beta)}\,|\downarrow\rangle$, leaves the beams for the B coupling phaseless while the left A beam is the only one carrying a phase. As a conclusion, the phase originally defined as ϕ accounts for all the effects that laser beam dephasing could have on the system.

Numerical simulations of the effect of a given phase ϕ for the final achievable temperature and the cooling rate are shown in fig. 9 and 10. The truncation values puts a limit to the accuracy of the results when they get closer to the maximum occupation number. Thus, for the final temperature results, any value of the final occupation over 5 is to be taken as unreliable. If the incidence angle of the A coupling is the same as for the B coupling it is very likely that both beams follow a much more similar path and that phase effects can be controlled much better.

In addition, for the "Fano resonance" alternative of implementation, these effects are going to be less relevant. It is possible to phase lock a microwave and a laser field so that phase mismatches are reduced to a minimum.

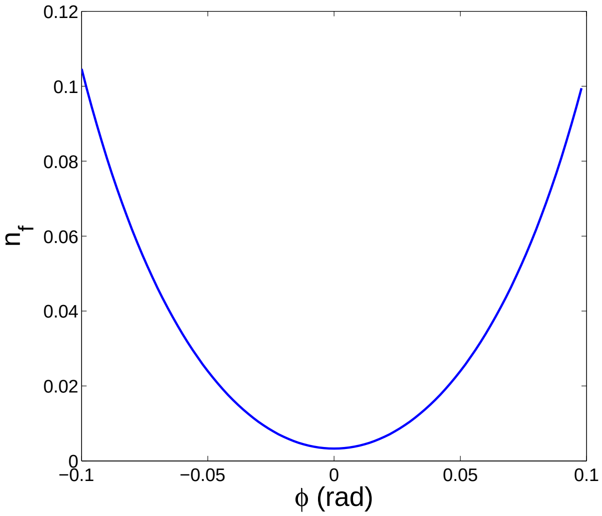

FIG. 9. Effect on final temperature of dephasing of one of the beams ($\Omega_B = 5\nu$, $\Omega_A = 400\nu$, $\Gamma = 15\nu$, $\eta_B = 0.1$).

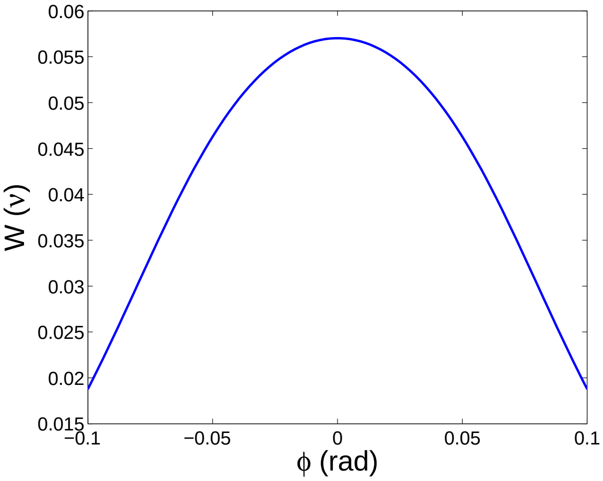

FIG. 10. Effect on final temperature of dephasing of one of the beams ($\Omega_B = 5\nu$, $\Omega_A = 400\nu$, $\Gamma = 15\nu$, $\eta_B = 0.1$).

IX. MULTI-MODE COOLING

The cooling scheme has also been tested for an ion chain using Monte Carlo simulation [24, 25]. The robustness of the scheme implies a wide range of operational Rabi frequencies or, in a different perspective, a wide range of trap frequencies for a given Rabi frequency. Thus, a particular central mode frequency can be addressed so that also the neighboring modes benefit from the cooling. Numerical test have been performed in a multi-mode environment with up to 3 ions and promising results have been obtained.

Quantum jumps method, also called Monte Carlo

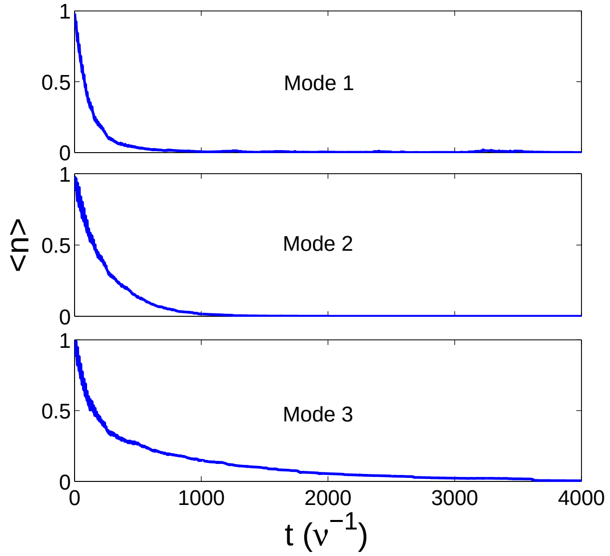

FIG. 11. 3 mode cooling where mode 2 is addressed. While the cooling is fast and to a low temperature in all modes, neighbouring modes 1 and 3 see a slight decrease in cooling efficiency ($\Omega_B = \nu$, $\Omega_A = 2.3\nu$, $\Gamma = 15\nu$, $\eta_B = 0.1$, with ν the eigenfrequency of the second mode).

wave-function method, is a useful tool to simulate the performance of our Robust cooling scheme in a multi-mode environment. A benefit from this method is found mainly for a system with a large number N of states, since it is equivalent to a master equation approach to an open system while still using the pure state formalism, thus reducing the number of tracked variables from N^2 to N. It is based on evolution with a non-Hermitian Hamiltonian and random quantum jumps, followed by wave-function renormalization to account for the non unitary evolution of the non-Hermiticity. The time step δt that can be used is lower bounded by the correlation time of the reservoir and upper bounded by the limitation $\eta_i \delta t \ll 1$, with η_i the eigenvalues of the Hamiltonian. At the time of simulating, a time step that allows for a quantum jump with a probability of roughly 10% is a good benchmark.

A simulation code has been developed that applies this method to a system composed by a chain of three level ions in a harmonic potential. It has been tested and benchmarked with side-band cooling of a single ion and then simulations were performed for three level systems as instances of EIT cooling, Stark-shift cooling and the proposal on this report. Observations led to the conclusion that our proposal is able to transfer the cooling ability to neighboring modes much more efficiently than other schemes, although as expected cooling rates and final temperatures are not as good as for the central mode. An instance of this performance is shown in Fig.11.

X. ATOM CLOUD COOLING

If Bose-Einstein condensation could be obtained by an all-optical means instead of evaporative cooling, higher densities could be obtained, since it would be possible to keep most of the initial atomic sample in the trap. The longer life of the sample would allow for recooling at the end of the experiment since it is a non-destructive procedure.

When, instead of a single atom, it is a collection of atoms that is to be cooled, the photons emitted by one atom can be reabsorbed by the next one, giving rise to heating mechanisms that need to be accounted for in the theoretical description. Independently to photon reabsorption, the emission lineshape of an atom is also affected by the presence of other atoms in what is called the phenomenon of superradiance. These processes, known globally as dipole-dipole interactions, become significant when the distance between particles is of the order of the transition wavelength. Their effect is to disturb the equilibrium conditions of the cooling scheme, making it less effective than in the one-particle case and acting as an independent heat source with an intrinsic heating rate. Thus, trials with sideband cooling in optical lattices [5] never reached sufficiently low temperatures to guarantee condensation. Our proposal is predicted, nevertheless, to reach null temperature up to second order in the Lamb-Dicke parameter with low effect of the parametric fluctuation. In addition, this scheme has a faster cooling rate. This would facilitate counteracting the effect of dipole-dipole interaction by cooling faster and to a lower temperature, and make the goal of Bose Einstein condensation by laser cooling a step closer.

Adapting the implementation proposal of Fig.6 to a trapping and cooling set up following [5] is relatively straightforward. Since the beams reproducing coupling B are highly detuned, they can also be used as the trapping light. Instead of a pair of counterpropagating beams, a set of three coplanar beams forming angles of 120^o with each other will generate an hexagonal dipole lattice. Geometric considerations demonstrate that the projection of the three wavevectors on any axis of the lattice plane yields two wavevectors of opposite sign and same module, so that any axis on the trap plane will see the same pair of two counterpropagating beams of Fig.6.

Although the harmonic wells forming the lattice are not strictly isotropic, they can be considered so in the neighborhood of the minimum. This is a correct assumption bearing in mind that the system resides in the Lamb-Dicke regime. This simplifies the implementation of the A coupling to the extent that it will have the same form of coupling B but for the fact that its plane needs to be tilted with respect to the trap in an angle such that satisfies condition in Eq.6. Starting from a configuration parallel to that of coupling B, the tilting needs to be done with respect to the perpendicular of one of the trapping beams.

This setup has the advantage that the axis perpendic-

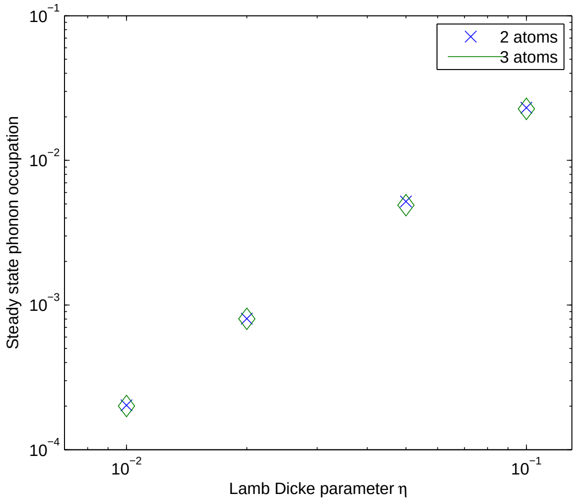

FIG. 12. Numerical simulation of the steady state population for a group of 2 and 3 atoms. ($\Omega_B = \nu$, $\Omega_A = 8.5\nu$, $\Gamma = 10\nu$, $\Delta = 2.5\nu$).

ular to the trap will only be mechanically affected by the beams of the A coupling, so that sideband cooling can be implemented on that axis. The possibility of implementing the present cooling proposal also on this vertical axis would only require two counter-propagating beams of type B parallel to the vertical axis.

This combination of cooling and trapping light converts it into a fairly simple experimental setting with a promising performance.

A numerical simulation following the approach of [26] has been performed where the scheme was applied to a group of 2 and 3 atoms, obtaining results that differ little from the case of a single particle. Both dipole-dipole and superradiance terms were taken into account. The main difference with the single atom model is the presence of the so-called bosonic-enhancement factors. The presence of many atoms in the same state enhances the couplings between levels. This has the effect of increasing the rate of interaction, but also of broadening absorption and emission lines. For schemes relying on resonance effects, like sideband cooling, this broadening is very detrimental. In our case, both carrier transition and blue sideband are under the influence of dark states and hence are not affected by this broadening. This is shown in Fig.12, where no difference in the steady state occupation values shows for increasing number of atoms. For this, the experimental values appearing in [5] have been taken. Since the trapping light is the same as that of coupling B, $\Omega_B \simeq \nu$. This requires $\eta_B = 4\eta_A$, which corresponds to a tilting angle of 60^o. Cesium atoms can be used for which the linewidth of the excited state is $\Gamma = 10\nu$. We believe this scheme could hence reduce the reachable temperature by laser means in atom clouds, bringing BEC by all-optical means a step closer.

XI. CONCLUSIONS

A detailed study of a robust and fast laser cooling scheme for trapped three level systems has been presented. It has been shown that a particular setting of the Lamb-Dicke parameters ratio combines two underlying cooling schemes so that the eigenspace dimension of final steady states is reduced to one. Thus, the ground state is reached up to second order in the Lamb-Dicke expansion. Being both a fast and a robust cooling scheme, two different experimental implementations have been proposed that equivalently perform the scheme. An equally simple implementation would be able to also cool the two resting axis, thus converting it into a 3D cooling scheme without further changes in the experimental setup. It has been demonstrated that the robustness and fast cooling rate would make it suitable for cooling of several ions in a trap or of a cloud of atoms in an optical lattice, bringing BEC condensation with laser cooling closer to a factible goal.

ACKNOWLEDGMENTS

This work was supported by the AXA Research Fund, EU STREP projects HIP and PICC, the GIF project "Non-linear dynamics in ultra-cold trapped ion crystals" as well as the Alexander von Humboldt foundation.

---

[1] J. Cerrillo, A. Retzker, and M. B. Plenio, Phys. Rev. Lett. **104**, 043003 (2010).
[2] S. Chu, Rev. Mod. Phys. **70**, 685 (1998).
[3] C. N. Cohen-Tannoudji, Rev. Mod. Phys. **70**, 707 (1998).
[4] W. D. Phillips, Rev. Mod. Phys. **70**, 721 (1998).
[5] V. Vuletić, C. Chin, A.J. Kerman, and S. Chu, Phys. Rev. Lett. **81**, 5768 (1998).
[6] T. Hänsch and A. Schawlow, Opt. Commun. **13**, 68 (1975).
[7] D. Wineland and H. Dehmelt, Bull. Am. Phys. Soc **20**, 637 (1975).
[8] D. J. Wineland, R. E. Drullinger, and F. L. Walls, Phys. Rev. Lett. **40**, 1639 (1978).
[9] A. Aspect, E. Arimondo, R. Kaiser, N. Vansteenkiste, and C. Cohen-Tannoudji, Phys. Rev. Lett. **61**, 826 (1988).
[10] R. Dum, P. Marte, T. Pellizzari, and P. Zoller, Phys. Rev. Lett. **73**, 2829 (1994).
[11] I. Marzoli, J.I. Cirac, R. Blatt, and P. Zoller, *et al.*, Phys. Rev. A **49** 2771 (1994);
[12] C. Monroe, D.M. Meekhof, B.E. King, S.R. Jefferts, W.M. Itano, D.J. Wineland, and P. Gould, *et al.*, Phys.

Rev. Lett. **75** 4011 (1995).
[13] M. Fleischhauer, A. Imamoglu, and J. P. Marangos, Rev. Mod. Phys. **77**, 633 (2005).
[14] G. Morigi, J. Eschner, and C. H. Keitel, Phys. Rev. Lett. **85**, 4458 (2000).
[15] C. F. Roos, D. Leibfried, A. Mundt, F. Schmidt-Kaler, J. Eschner, and R. Blatt, Phys. Rev. Lett. **85**, 5547 (2000).
[16] A. Retzker and M. B. Plenio, New J. of Phys. **9**, 279 (2007).
[17] D. Jonathan and M. B. Plenio, Phys. Rev. Lett. **87**, 127901 (2001); D. Jonathan, M. B. Plenio, and P. L. Knight, Phys. Rev. A **62**, 042307 (2000).
[18] M. Lindberg and J. Javanainen, J. Opt. Soc. B **3**, 1008 (1986).
[19] J. Javanainen and S. Stenholm, Applied Physics A **24**, 151 (1981).
[20] J. I. Cirac, R. Blatt, P. Zoller, and W.D. Phillips, Phys. Rev. A **46**, 2668 (1992).
[21] F. Mintert and C. Wunderlich, Phys. Rev. Lett. **87**, 257904 (2001).
[22] N. Timoney I. Baumgart M. Johanning A.F. Varon Ch. Wunderlich M.B. Plenio and A. Retzker, Nature **476**, 185 (2011).
[23] P. Rabl, P. Cappellaro, M. V. G. Dutt, L. Jiang, J. R. Maze, and M. D. Lukin, Phys. Rev. B **79**, 041302(R) (2009).
[24] K. Mølmer, Y. Castin, and J. Dalibard, J. Opt. Soc. Am. B **10**, 524 (1993).
[25] M. B. Plenio and P. L. Knight, Rev. Mod. Phys. **70**, 101 (1998).
[26] L. Santos and M. Lewenstein, Phys. Rev. A **60**, 3851 (1999).
[27] D. F. James and J. Jerke, Can. J. Phys. **85**, 625 (2007).

Appendix A: Diagonalization of two Discrete States and a Continuum

Let us first consider the manifold $\{|e\rangle, \{|+,1\rangle\}, \{|-,1\rangle\}\}$. This can be diagonalized to generate the continuum $\{|k'\rangle\}$. Through $|e\rangle$, the bright state $|+\rangle$ also couples to the continuum $\{|k'\rangle\}$ with the term $\frac{\Omega_A}{\sqrt{2}}\langle e|k'\rangle\,\sigma_x^{(+,k')}$. Let us now consider how the excited state overlaps with the continuum $\{|k\rangle\}$ originated in the manifold $\{|+\rangle, \{|k'\rangle\}\}$. The Hamiltonian H_k that appears diagonal to $|k\rangle$ can be split into $H_{k'}$, which is diagonal for $|k'\rangle$ and the coupling to the state $|+\rangle$. It satisfies:

$$\begin{aligned} H_k\,|k\rangle &= \left[H_{k'} + \Omega_B\,|+\rangle\langle+| + \frac{\Omega_A}{\sqrt{2}}\sigma_x^{(+,e)}\right]|k\rangle \\ &= k\,|k\rangle . \end{aligned} \tag{A1}$$

Projection onto $|k'\rangle$ and $|+\rangle$ yields:

$$k'\,\langle k'|k\rangle + \frac{\Omega_A}{\sqrt{2}}\,\langle k'|e\rangle\,\langle +|k\rangle = k\,\langle k'|k\rangle \tag{A2}$$

$$\Omega_B\,\langle +|k\rangle + \frac{\Omega_A}{\sqrt{2}}\int \langle e|k'\rangle\,\langle k'|k\rangle\,dk' = k\,\langle +|k\rangle \tag{A3}$$

From (A2) the following expression is obtained:

$$\langle k'|k\rangle = \frac{\Omega_A}{\sqrt{2}}\frac{1}{k-k'}\,\langle k'|e\rangle\,\langle +|k\rangle\,, \tag{A4}$$

which can be substituted in (A3) to obtain:

$$\left(\frac{\Omega_A}{\sqrt{2}}\right)^2 \int \frac{|\langle e|k'\rangle|^2}{k-k'}dk' = (k-\Omega_B)\,. \tag{A5}$$

Now the overlap $\langle e|k\rangle$ can be calculated:

$$\begin{aligned} \langle e|k\rangle &= \int \langle e|k'\rangle\,\langle k'|k\rangle\,dk' \\ &= \frac{\Omega_A}{\sqrt{2}}\int \frac{|\langle e|k'\rangle|^2}{k-k'}\,\langle +|k\rangle\,dk' \\ &= \frac{\sqrt{2}}{\Omega_A}\,(k-\Omega_B)\,\langle +|k\rangle \end{aligned} \tag{A6}$$

Appendix B: Effective Coupling of the Ground States

In this section the relationship between the physical Lamb-Dicke parameter η_p and the effective η_B is derived. The method in [27] is followed, where the highly detuned excited level is adiabatically eliminated. Our target Hamiltonian describing the coupling of both ground levels is the following:

$$V_{SSh} = \frac{\Omega_B}{2}\left(\sigma_x^{(\uparrow,\downarrow)} + \eta_B\sigma_y^{(\uparrow,\downarrow)}\hat{q}\right) \tag{B1}$$

The experimental implementation involving a highly detuned Raman coupling is described by the following interaction picture Hamiltonian:

$$\begin{aligned} H_I = \frac{\Omega_p}{2}(&|e\rangle\langle\uparrow|e^{i\Delta t}(1+i\eta_p(b^\dagger e^{-i\nu t}+be^{i\nu t})) \\ &+|e\rangle\langle\downarrow|e^{i\Delta t}(1-i\eta_p(b^\dagger e^{-i\nu t}+be^{i\nu t}))+h.c.). \end{aligned} \tag{B2}$$

This Hamiltonian consists of the following harmonic terms:

$$\begin{aligned} h_1 &= \frac{i\Omega_p\eta_p}{2}(|e\rangle\langle\uparrow| - |e\rangle\langle\downarrow|)b^\dagger \\ h_2 &= \frac{\Omega_p}{2}(|e\rangle\langle\uparrow| + |e\rangle\langle\downarrow|) \\ h_3 &= \frac{i\Omega_p\eta_p}{2}(|e\rangle\langle\uparrow| - |e\rangle\langle\downarrow|)b \end{aligned} \tag{B3}$$

with frequency values $\omega_1 = \Delta - \nu$, $\omega_2 = \Delta$ and $\omega_3 = \Delta+\nu$. The derivation of the effective Hamiltonian follows the formula:

$$H_{eff}(t) = \sum_{m,n=1}^{3} \overline{\omega_{mn}}^{-1}\left[h_m^\dagger, h_n\right]\exp[i(\omega_m-\omega_n)t], \tag{B4}$$

where $\overline{\omega_{mn}}$ is the harmonic average $\overline{\omega_{mn}}^{-1} = 1/2(\omega_m^{-1} + \omega_n^{-1})$. Of the nine terms originating from this expression, four of them are of second order in the Lamb-Dicke parameter. The remaining six can be expressed as:

$$\begin{aligned} H_{eff} =& \nu a^\dagger a + \frac{\Omega_p^2}{4}\frac{1}{\Delta}(\sigma_z^{(\uparrow,e)} + \sigma_z^{(\downarrow,e)} + \sigma_x^{(\uparrow,\downarrow)}) \\ &+ \frac{\Omega_p^2 \eta_p}{4}\frac{2\Delta^2 - \nu^2}{\Delta(\Delta^2 - \nu^2)}\hat{q}\sigma_y^{(\uparrow,\downarrow)} \\ &+ \frac{\Omega_p^2 \eta_p}{4}\frac{\nu}{\Delta^2 - \nu^2}\hat{p}\sigma_z^{(\uparrow,\downarrow)}. \end{aligned} \tag{B5}$$

where $\hat{p} = i(b - b^\dagger)$. This Hamiltonian is equivalent to (B1) but for the atomic Stark shifts and the last term, which is proportional to $1/\Delta^2$.

As long as $\Delta \gg \nu$, H_{eff} contains the target interaction V_{SSh} with the parametric conditions:

$$\begin{aligned} \frac{\Omega_B}{2} &= \frac{\Omega_p^2}{4\Delta} \\ \frac{\Omega_B \eta_B}{2} &= \frac{\Omega_p^2}{4\Delta}\eta_p \frac{2\Delta^2 - \nu^2}{\Delta^2 - \nu^2} \end{aligned} \tag{B6}$$

Solving for the Lamb-Dicke parameter:

$$\eta_B = \eta_p \frac{2\Delta^2 - \nu^2}{\Delta^2 - \nu^2} \tag{B7}$$

which yields $\eta_B = 2\eta_p$ for the assumed limit $\Delta \gg \nu$. If we take the fluctuations optimal point $\Omega_B = \nu$, the condition becomes $\eta_p/\eta_A = 2$. This can be achieved for a layout where beam p is colinear to the trap axis and beam A, with a very similar frequency, is 60^o away from the axis.